International Journal of Current Research in Multidisciplinary (IJCRM) *ISSN: 2456-0979*
Vol. 5, No. 8, (August'20), pp. 06-11

STUDY OF THE PHOTO CATALYTIC EFFECT OF ZINC OXIDE NANO PARTICLES PREPARED BY HYDROTHERMAL METHOD

Omima.K.Hussein [1,*], Asmaa.M.Raslan[2]
[1,2]*Al-Azhar University, Faculty of Science (Girls), Chemistry Department, Nasr City, Cairo, Egypt*

ABSTRACT
ZnO nanoparticles have been prepared by a hydrothermal method and characterized by Transmission Electron Microscopy(TEM), X-Ray Diffraction(XRD),and Energy-dispersive analysis X-ray spectra(EDX).And we have studied the photocatalytic behavior of the ZnO nano-particles,The characterization results show that the particle size of the as prepared-zinc oxide is in the nanometre range. According to XRD characterization, the average particle size of zinc oxide prepared has been determined using Scherrer's equation.The average of the size particles of zinc oxide was 42.8nm, and when we applied the prepared-ZnO photocatalyst on AR18 at different pH values we found that the photodegradation is highest at pH = 5.
KEYWORDS: *nanomaterials, ZnO,semiconductor, photocatalyst*

INTRODUCTION

Heterogeneous photocatalysis by semiconductors for the removal of pollutants and the generation of hydrogen has been revealed as of its importance in the ecological management and to grow renewable energy [1,2]. Numerous semiconductor photocatalysts of metal oxides, for example, TiO_2, ZnO, WO_3 and, α-Fe_2O_3, have been repeatedly discovered for their brilliant photocatalytic enactment [3,4]. As a public semiconductor, ZnO materials have been prepared and settled as favorable photocatalysts with several nanostructures [5,6,7]. In many cases, the use of ZnO depended on its direct wide bandgap (3.37 eV) and the large excitation binding energy (60 mV) at room temperature [8].

The current study focus on the hydrothermal production of ZnO nanoparticles, and the effect of time of growth on its properties. The hydrothermal synthesis of ZnO powders has four advantages (1) powders with nanometer- size can be formed by this method (2) the reaction is carried out under adequate conditions (3) powders with different morphologies by adjusting the reaction conditions and (4) the as-prepared powders have different properties from that of the bulk.

EXPERIMENTAL DETAILS

The starting materials, zinc acetate dihydrate ($Zn(CH3COO)_2 \cdot 2H_2O$, purity >99.5%, Merck), sodium hydroxide (NaOH, purity 98%, Kemika) and polyvinylpyrrolidone (PVP, $(C_6H_9NO)n$, purity 99%, Sigma–Aldrich) as a polymer surfactant, were used as received from the manufacturers, without any treatment [9].

We mix 2.7463 g (0.01 mol) of zinc acetate dihydrate and 0.0574 g (2×10^{-6} mol i.e. 5 wt%) of PVP and then dissolved in 750 ml of deionized water with constant stirring at 1000 rpm and heat at 80^0C. After the dissolution of zinc acetate dihydrate and PVP, an amount of NaOH solution was introduced to adjust the pH range (pH 10 –11) resulting in a white precipitate. And then the prepared suspension was thermally treated up to 120^0C at a constant heating rate of 20^0C /min, under constant stirring of 400 rpm. The reaction time was 72 h.

After cooling at room temperature, the products were taken out and washed with deionized to remove some existing ions and impurities. The final products were dried at 80^0C. The white precipitates then calcined at 450^0CThe XRD patterns were examined using a Shimadzu Diffractomater x D-D1. Series with monochromatizedCuKα radiation (λ = 1.5418 Å). The initiator was operated at 40 kV and 25 mA. The samples were scanned at a diffraction angle from 10 to 80° at the scanning rate of 0.068°/s. Morphological notes were performed on transmission electron microscopy (TEM) (JEM-100 CX (JEOL Ltd.). UV-9200 UV/VIS spectrophotometer.

The chemical compositional analysis of the pure ZnO has been carried out using OXFORD link ISIS Energy Dispersive X-ray Spectroscopy.

RESULTS AND DISCUSSION

3.1- X-Ray diffraction (XRD)

The XRD of the synthesized zinc oxide shows broad peaks at values of 31.77, 34.40, 36.22, 47.50, 56.60, 62.63, 66.39, 67.95, 69.06, 72.56, and 76.97 which can be assigned to diffraction from: 100, 002, 101, 102, 110, 103, 200, 112, 201, 004, and 202 crystal planes, respectively [10]. A concentrated ZnO {101} peak was detected signifying that the ZnO favored progression in this direction. the broadening of the line of the diffraction peaks is a signal of that the synthesized ZnO is in nanometer size. The average particle size has been calculated from a full width at half maximum (FWHM) of the diffraction peaks by use of the equation of Scherrer's eq.(1):

$D=k\lambda/\beta\cos\theta$(1)

Since λ is the wavelength of x-ray and β is the full width at half maximum. The average particle size of zinc oxide nanoparticles has been established to be 42.8nm

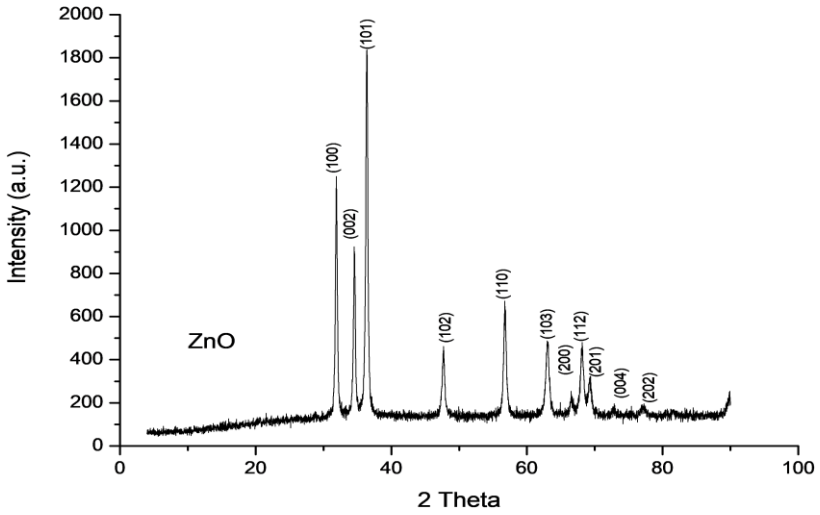

Figure 1:XRD patterns of ZnO at 450^0C

3.2-Transmission electron microscope (TEM)

Figure (2) show the TEM of ZnO at a calcinations temperature of 450^0C. it shows small nanorods and small nanospheres with a smooth surface.

Agreeing with the Erwin model and about the oriented attachment mechanism, the growth process of ZnOnanocrystal obeys the nucleation–absorption– orientation–coalescence mechanism. In the growth process of pure ZnOnanocrystal, the positive terminal of Zn-(0001) plane of one growth unit coalesces with the negative terminal O-(0001) plane of another growth unit, the surface charges are compensated [11,12], also, the growth process is easily ended and as a result, short ZnO nanoparticles

are produced. Furthermore, the ZnO growth may be explained due to the chemical reactions which occur and the growth of the crystals of ZnO [13]. Their action process can be explained as the following :

$$Zn^{2+} + 4OH^{-} \rightarrow Zn(OH)_2\downarrow \quad (2)$$

$$Zn(OH)_2 + 4OH^{-} \rightarrow Zn(OH)^{2-}_4 \quad (3)$$

$$Zn(OH)^{2-}_4 \rightarrow ZnO + H_2O + 4OH^{-} \quad (4)$$

The last reaction (3) might be noticed if we Put (NaOH) to the solution of Zn^{2+} ions. And after the addition of more NaOH solution, $Zn(OH)_2$ precipitate would be liquefied to form a uniform solution having Zn(OH)2−4 ions. Then by the time, ZnO nuclei shaped from the dryness of $Zn(OH)^{2-}4$ ions and followed by the growth of the crystals. Commonly, ZnO crystals formed in the structure of hexagonal wurtzite that are polar as the Zn ions and O ions join together over tetrahedral coordination, which gave the polar symmetry along the hexagonal axis. It was clear that two plans that are polar for ZnO crystallites: one is the positively polar plane ended by Zn(0001) and the other is the negatively polar plane ended by O(0001−). ZnO plane which ended by Zn is catalytically active but the plane that ended by O is unmotivated [14]. Furthermore, the growing custom has been governed by the speed of the growth of different planes in the ZnO crystal. Laudise and Ballman stated that as the growth is higher, the disappearance of the plane would be faster, which gives rise to the pointed shape on the end of the c-axis [15]. In ZnO, the growth speed of the ZnO plane in different directions were [0001]> [011−1−] > [011−0] > [011−1] > [0001−] [16]. so, the ZnO crystallites grow very fast along [0001] direction (c-axis), which give rise to the formation of nano rod-like structure.

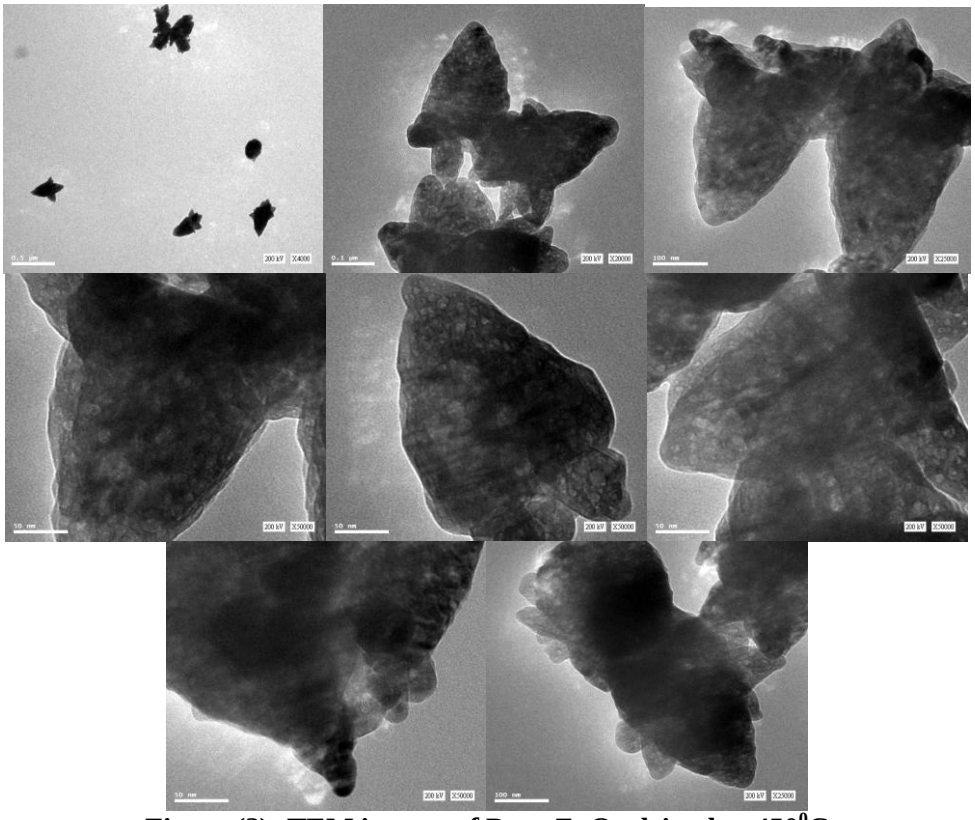

Figure (2): TEM images of Pure ZnOcalcined at 450^0C

3.3-Energy-dispersive analysis X-ray spectra (EDX)

The chemical compositional analysis of the pure ZnO have been carried out using EDX as shown Figure (3)

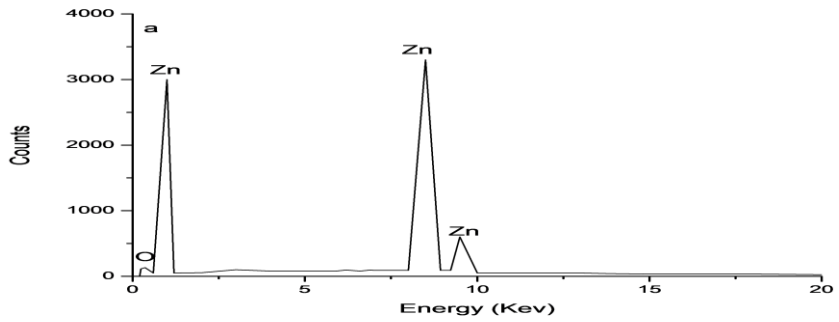

Figure (3) : EDX of pure ZnO burned at 450^0C

4-Photocatalytic activity of ZnO :

Effect of solution's pH:

The effect of solution pH on photocatalytic degradation of AR18 with ZnO was studied by changing the initial pH of aqueous AR18 solution from 2.0 to 10.0 with aqueous HCl or NaOH solutions while keeping all other experimental conditions constant. The absorption is considered to be in linear proportion with the concentration of AR18 regarding the equation (5) [17].

$C/C_0 = A/A_0$ (5)

Besides, The degradation effectiveness was calculated using the equation (6) [18]:

Degradation % (D%)= $((C_0\text{-}C)/C_0)\times100=((A_0–A)/A_0)\times100$ (6)

where C_0 represents the initial concentration, C signifies the changed concentration; A0 signifies the initial absorbance, and A signifies the changing absorbance of the AR18 at the characteristic absorption wavelength of 510 nm.

as shown in figures (4.a, 4. b, 4.c and 4.d)show the Plot of absorbance at λmax (510 nm) vs. time for AR18 with ZnO, The apparent reaction rate constants (kap) for photocatalytic degradation of AR18 dye, the photocatalytic degradation of AR18 dye vs time, and the relationship between the kap value and solution pH respectively for dye concentration [AR18] = 1.0×10^{-5}M at different pH values. Figures show that photocatalytic degradation was increased with increasing the value of pH and the best resultwasobtainedaround pH=5.0.

Figure (4.d) is estimated from experimental data using linear regression. The slopes of the straight lines passing through the origin gave the apparent rate constants (*k*ap) showed in Table (1), we notice that *r* (correlation coefficient) values are greater than 0.98, which approve the proposed kinetics for decolorization of dye in this process.

, the Langmuir–Hinshelwood (L–H) kinetic equation is one of the most useful models to describe this type of reaction model modified to accommodate reactions occurring at a solid-liquid interface [19]. The photocatalytic reaction rate is given by Eq. (7):

$$r = - dC_s/dt =(k_rKC_s)/(1 + KC_s) \quad (7)$$

here r is the rate of reaction, C_S is substrate (AR18) concentration, t is the time of the reaction, k_r is the reaction rate constant and K is the adsorption constants associated with the substrate. When the pollutant concentration is very low, the term KC_S is negligible and by using $k_rK = k_{ap}$, the apparent reaction rate becomes a pseudo-first-order reaction Eq. (8). $-\ln C_t/C_0= k_{ap}t$ (8)

where k_{ap} is the apparent pseudo-first-order rate constant (min^{-1}) and C_0 and C_t are the concentrations of AR18 at initial and given reaction time (min), respectively. The resulting pseudo-first-order rate constant has been used to calculate the degradation rate for AR18 and is used for a comparison of the efficiency of the photocatalytic process. The semi-logarithmic graphs in the presence of ZnOversus irradiation time loading yield straight lines indicating pseudo-first-order reaction.

The degradation efficiency steadily increased with increasing reaction time at all tested pH values After 40 min, the degradation efficiencies of ZnO increased from 8.33 % to 93.33 when the pH value increased from 2.0 to 5.0, while the degradation efficiencies dropped with the further increase in pH to 10.0 and this may be attributed to that:

At a low pH, AR18 was mainly in its neutral unionized form and the surface of ZnO was positively charged. For pH 2.0, the pH was adjusted by HCl, while the Cl^- anions might have been adsorbed on the surface of the catalyst [20, 21]. This has been confirmed by Liang et al. [20] that a struggle between the adsorption of the Cl^- anions and substrate molecule would occur on the catalyst surface to lower the photocatalytic activity. Nevertheless, at pH 5.0, the Cl^- anions did not exist because the pH did not need the adding of any HCl to adjust the pH solution. Accordingly, the electrostatic attraction between positively charged ZnO with AR18 molecules resulted in high degradation efficiency of AR18.

On the other hand, at higher pH, as AR18 molecules experienced de-protonation and became negatively charged, their adsorption was also predictable to be affected by an increase in the density of ZnO− groups on the catalyst surface. Thus, due to Coulombic repulsion, the AR18 was barely adsorbed [22]. also, the pH was adjusted by NaOH for higher pH value. Bekkouche et al., [2004][23] had reported that the adsorption of ions from NaOH salt may produce a struggle with the substrate molecules on the surface of the catalyst, also leading to lower photocatalytic activity. Taking into account of above-mentioned details, the best solution pH was 5.0, which was the natural value of the aqueous AR18 solution.

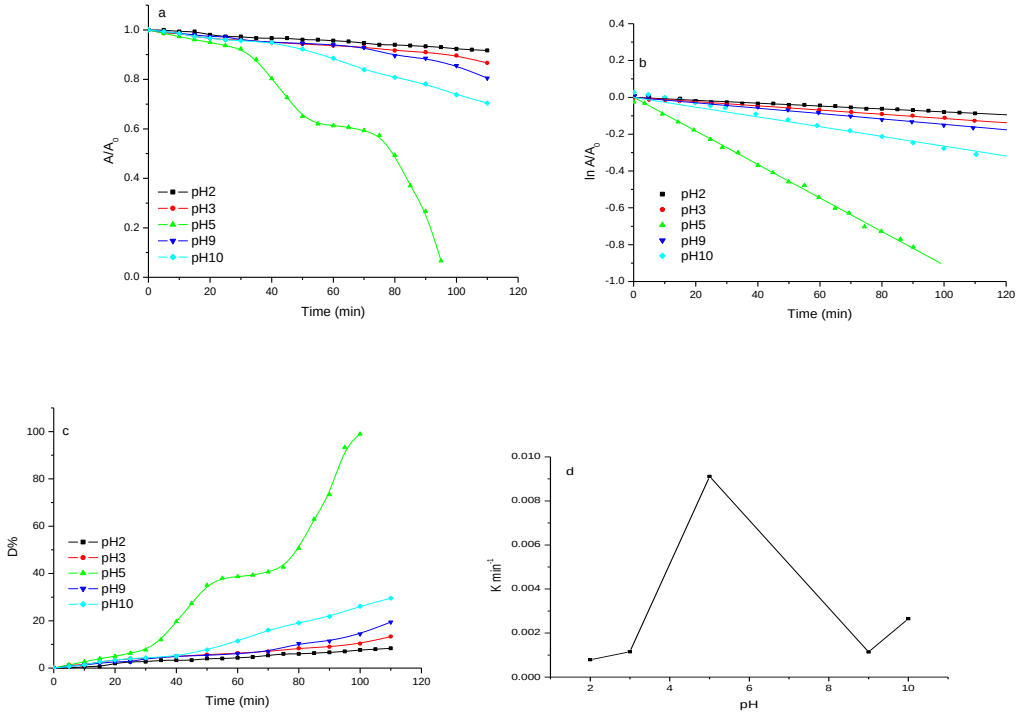

Figure 4: (a) Plot of absorbance vs. time , (b) Kinetics of photodegradation for AR18 with ZnO,(c) D% of photodegradation for AR18 with ZnO and (d) Plot of k (min^{-1}) vs. time for AR 18 with ZnOcalcined at450^0C at different pH values. [AR18] =1.0×10^{-5}M.

Table (1): Kinetics of photodegradation of AR18 onto ZnOcalcinedat 450^0C at different pH values , [AR18] =1.0×10^{-5}M.

pH	D%	$k\times10^{-3}$ (min^{-1})	R
2.0	8.33	0.78	0.9920
3.0	13.33	1.15	0.9980
5.0	93.33	9.11	0.9998
9.0	19.46	1.14	0.9993
10.0	29.53	2.56	0.9993

CONCLUSIONS

ZnO nanoparticles have been prepared by a hydrothermal method and characterized by Transmission Electron Microscopy(TEM), X-Ray Diffraction(XRD),and Energy-dispersive analysis X-ray spectra(EDX).And we have studied the photocatalytic behavior of the ZnO nano-particles,The characterization results show that the particle size of the as prepared-zinc oxide is in the nanometre range. According to XRD characterization, the average particle size of zinc oxide prepared has been determined using Scherrer's equation.The average of the size particles of zinc oxide was 42.8nm, and when we applied the prepared-ZnO photocatalyst on AR18 at different pH values we found that the photodegradation is highest at pH = 5.

REFERENCES

[1] Y-F. Cheng, W.Jiao, Q. Li, Y. Zhang, S. Li, D. Li, R. Che, Journal of Colloid and Interface Science, 509 (2018) 58–67.

[2] R. Su, N. Dimitratos, J.J. Liu, E. Carter, S. Althahban, X.Q. Wang, Y.B. Shen, S. Wendt, X.D. Wen, J.W. Niemantsverdriet, B.B. Iversen, C.J. Kiely, G.J. Hutchings, F. Besenbacher, ACS Catal., 6 (2016) 4239–4247.

[3] Q. Guo, C.Y. Zhou, Z.B. Ma, Z.F. Ren, H.J. Fan, X.M. Yang, Chem. Soc. Rev., 45 (2016) 3701–3730.

[4] P.Y. Dong, G.H. Hou, X.G. Xi, R. Shao, F. Dong, Environ. Sci.Nano, 4 (2017) 539–557.

[5] Z. R. Tian, J. A. Voigt, J. Liu, B. Mckenzie, M. J. Mcdermott, M. A. Rodriguez, H. Konishi, H.F. Xu, Nat. Mater., 2 (2003) 821–826.

[6] L. Q. Jing, W. Zhou, G. H. Tian, H. G. Fu, Chem. Soc. Rev., 42 (2013) 9509–9549.

[7] A. Wei, L. Pan, W. Huang, Materials Science and Engineering B, 176 (2011) 1409.

[8] L. Wu, Y.Wu, Journal of Materials Science, 42 (2007) 406.

[9] L. X. Zhang, P. Liu, Z. Su, J Mol. Catal. A: Chem., 248 (2006) 189–197.

[10] A. F.M. Ismail, M. M. Ali, L. F.M. Ismail, Journal of Photochemistry and Photobiology B: Biology, 138 (2014) 99–108.

[11] J. Iqbal, X. Shan, G. Huang, H. Fu, R.Yu, D.Yu,. Mater. Chem. Phys., 113 (2009) 103– 106.

[12] Z. L.Wang, J. Phys: Condens. Matter, 16 (2004) R829– R858.

[13] J. Sin, S. Lam, K. Lee, A. Mohamed, Ceramics International, 39 (2013) 5833–5843.

[14] P. X. Gao, Z. L. Wang , J. Phys. Chem. B 108 (2004) 7534–7537.

[15] R. A. Laudise, A. A. Ballman, J. Phys. Chem., 64 (1960) 688–691.

[16] J. Yang, X. Li, J. Lang, L.Yang, M. Wei, M. Gao, J. Cao, Materials Science in Semiconductor Processing, 14 (2011) 247– 252.

[17] O.Yayapao, T. Thongtem, A. Phuruangrat and S. Thongtem, J Alloys and Compounds, 576(2013) 72-79.

[18] J. Xu, Y. Chang, Y. Zhang, S. Ma, Y. Qu, C. Xu, Appl. Surf. Sci. 255 (2008) 1996-1999.

[19]K. Naeem, F. Ouyang, Preparation of Fe^{3+}-doped TiO_2 nanoparticles and its photocatalytic activity under UV light, Physica B 405 (2010) 221–226.

[20] H.C. Liang, X.Z. Li, Y.H. Yang, K.H. Sze, Chemosphere 73 (2008) 805.

[21]M.L. Zhang, T.C. An, X.H. Hu, C. Wang, G.Y. Sheng, J.M. Fu, Appl. Catal. A: Gen. 260 (2004) 215.

[22]U.I. Gaya, A.H. Abdullah, M.Z. Hussein, Z. Zainal, Desalination 263 (2010) 176.

[23]S. Bekkouche, M. Bouhelassa, N. Hadj Salah, F.Z. Meghlaoui, Desalination 166 (2004) 355.